

SPINE: Token-Selective Test-Time Reinforcement Learning with Entropy-Band Regularization

Jianghao Wu^{1*}, Yasmeen George¹, Jin Ye¹, Yicheng Wu², Daniel F. Schmidt¹, Jianfei Cai¹

¹Monash University ²Imperial College London

Abstract

Large language models (LLMs) and multimodal LLMs (MLLMs) excel at chain-of-thought reasoning but face distribution shift at test-time and a lack of verifiable supervision. Recent test-time reinforcement learning (TTRL) methods derive label-free pseudo-rewards from self-consistency voting over sampled trajectories, yet they often collapse: the majority-vote reward prevails, responses shorten, and Pass@1 declines. We trace this to uniform sequence updates in which most tokens are low-entropy followers, while a small high-entropy subset determines the reasoning branches. Thus we propose SPINE, a token-selective test-time reinforcement learning framework that (i) updates only forking tokens, the high-entropy branch points identified from forward-pass statistics, and (ii) applies an entropy-band regularizer at those tokens to sustain exploration when entropy is too low and to suppress noisy supervision when it is too high. SPINE plugs into GRPO-style objectives, optionally with a KL anchor, and requires no labels or reward models. Across ten benchmarks spanning multimodal VQA, general and expert QA, mathematical reasoning, and medical QA, SPINE consistently improves Pass@1 over TTRL while avoiding response-length collapse and yielding more stable training dynamics on both LLM and MLLM backbones. These results indicate that aligning updates with chain-of-thought branch points is a simple and label-free mechanism for stable and effective test-time adaptation in reasoning models. Code is available at <https://github.com/JianghaoWu/SPINE>.

1. Introduction

Large-scale foundation models, including both language models (LLMs) and multimodal large language models (MLLMs), exhibit impressive chain-of-thought (CoT) reasoning across a wide range of general-domain tasks [8, 14, 48]. Yet real-world deployment faces two persistent pressures: *distribution shift at test-time* [11, 31, 59] and

the scarcity of verifiable supervision [3, 40]. Reinforcement learning with verifiable rewards (RLVR) can unlock stronger reasoning [22, 35], but it presupposes dense labels or high-quality reward models that many domains lack, e.g., mathematical problem solving [27], clinical decision support [42], and scientific QA [12]. These constraints motivate improving models directly on unlabeled test inputs rather than waiting for new annotations.

Test-Time Training (TTT) adapts models on incoming unlabeled data, typically via pseudo-labels or self-supervised signals [1, 2, 38, 39]. However, recent evidence indicates that reinforcement learning generalizes more robustly than supervised fine-tuning (SFT) on reasoning tasks, where SFT often imitates surface patterns rather than improving deductive behavior [28, 52]. Building on this, Test-Time Reinforcement Learning (TTRL) [67] and unsupervised post-training for MLLMs [49] sample multiple reasoning paths and derive pseudo-rewards via self-consistency voting (Fig. 1a), yielding substantial gains without labels or reward models. Nevertheless, in practice standard TTRL quickly develops a characteristic collapse mode. As updates proceed, the majority-vote reward keeps increasing while responses become shorter and Pass@1 eventually drops (Fig. 1b, top). This behavior suggests that the policy is optimizing agreement among sampled trajectories rather than correctness, converging to a small set of short, self-consistent but often incorrect answers. This collapse stems from learning on noisy pseudo-rewards: uniform sequence updates implicitly treat self-consistency as a faithful surrogate for correctness, thereby exposing a structural mismatch between the proxy signal and the true objective. These failure modes in turn suggest that updating all tokens uniformly may be fundamentally misaligned with where the reasoning actually branches.

Recent analyses of token-entropy patterns in CoT from RLVR reveal a highly skewed distribution: the vast majority of tokens are generated with low entropy, while only a small minority in the top quantiles ($\approx 20\%$) exhibit high entropy (Fig. 1c). The same study [46] shows that these high-entropy tokens act as branch points that steer the chain-of-thought, whereas low-entropy tokens mainly carry local

*Corresponding author. Email: jianghao.wu@monash.edu

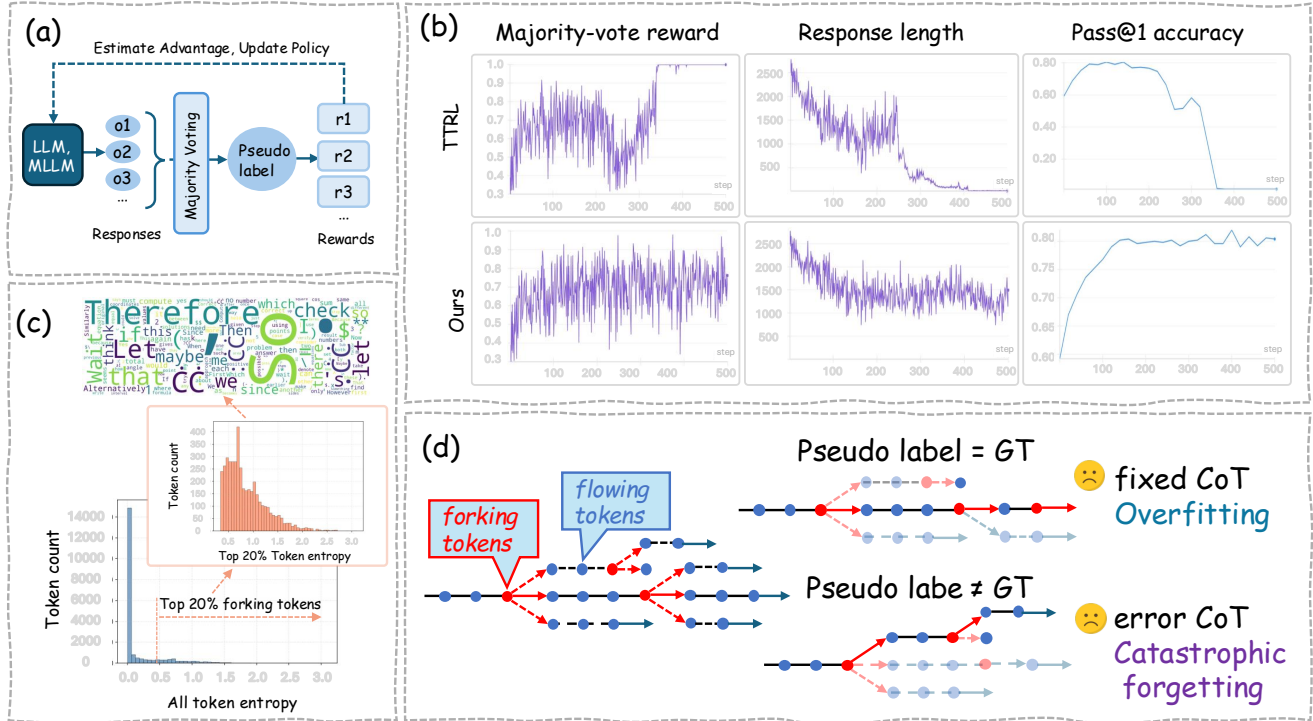


Figure 1. Motivation of SPINE. (a) TTRL: sample multiple responses, majority vote forms a pseudo-label, then update with GRPO. (b) TTRL is unstable with shrinking outputs. (c) Entropy is skewed; the top 20% high-entropy tokens mark forking decisions. (d) SPINE updates only forking tokens and applies an entropy band, stabilizing adaptation and mitigating overfitting and forgetting.

continuity. In our TTRL setting, we leverage this entropy-based view to a qualitatively different regime: *label-free test-time RL for reasoning* driven by noisy self-consistency pseudo-rewards. Rather than updating all tokens uniformly, we recast TTRL as exploration in the CoT decision space: high-entropy positions define a small set of *forking tokens* that form the reasoning “spine” along which adaptation should occur, whereas low-entropy follower tokens are better left unchanged to preserve stable local realizations. This token-selective view turns test-time optimization from full-sequence updates into sparse updates on forking tokens (Fig. 1d), concentrating gradients at actual decision points to prevent collapse, length shrinkage, and over-dispersion of the chain-of-thought under noisy pseudo-rewards.

We therefore propose SPINE (Selective Policy Improvements at Nodes of Entropy), a selective test-time reinforcement learning framework. (i) Token-selective updates. SPINE identifies forking tokens based on token entropy and applies GRPO-style policy updates only at these positions while preserving low-entropy follower tokens. (ii) Entropy-band regularization. It introduces a lightweight band-pass objective at forking tokens that increases entropy when too low to sustain exploration and decreases it when too high to suppress noisy supervision, thus preventing premature collapse. SPINE reuses forward-pass statistics (log probabili-

ties and entropies) and can include a KL anchor, requiring no labels or reward models.

Our main contributions can be summarized as follows.

- A token-selective TTRL paradigm that aligns updates with reasoning branch points (forking tokens) rather than with all tokens, preserving flowing segments.
- A band-pass entropy regularizer at forking tokens that jointly curbs collapse and over exploration, improving both stability and accuracy under noisy pseudo-rewards.
- Across *ten* benchmarks, SPINE consistently improves Pass@1 over TTRL on both LLM and MLLM backbones, while delivering more stable and reliable label-free test-time adaptation.

2. Related Work

2.1. Reasoning in LLMs and MLLMs

Reasoning in LLMs has been advanced mainly by supervised and self-supervised training that teach chain-of-thought (CoT), self-consistency, and reflection [47, 48]. Early LLMs internalize stepwise patterns via supervised fine-tuning (SFT) on (prompt, trace, answer) triplets, as in Flan-PaLM-style mixtures that enable zero-shot CoT [6, 60]. This SFT on CoT paradigm was then adopted by multimodal models. A common recipe first aligns vision

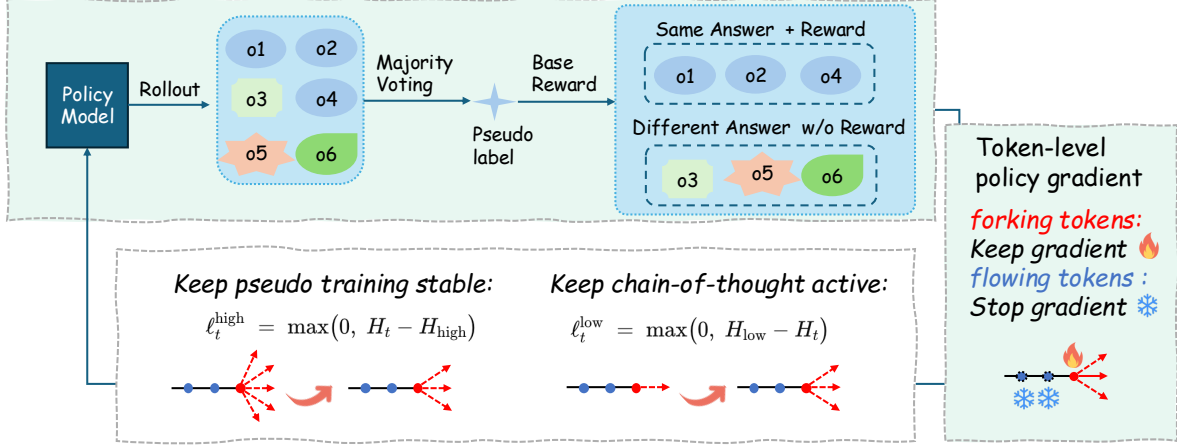


Figure 2. SPINE pipeline. The model samples responses, majority voting produces a pseudo-label, and rewards are assigned. Gradients update only forking tokens, while flowing tokens are frozen. An entropy band further stabilizes training and preserves reasoning diversity.

and language through visual instruction tuning, for example, LLaVA and MiniGPT-4, and then performs SFT on multimodal chain-of-thought data to elicit stronger visual reasoning, for example, LLaVA CoT and related systems [24, 54, 65]. These methods report consistent gains across visual math and chart understanding benchmarks. Despite its effectiveness, SFT behaves like behavior cloning of a single reasoning path, which can limit generalization and requires costly, high-quality reasoning traces [4, 7, 41]. These limitations motivate outcome-based reinforcement learning on tasks with verifiable solutions, where rewards are computed automatically by unit tests, checkers, or verifiers [20, 22]. Within this line, GRPO is a practical objective for long chain-of-thought: it is critic-free, estimates advantages from groups of rollouts, and yields a stable low-variance signal [35]. Building on GRPO, large reasoning models such as DeepSeekMath and the R1 series show strong gains on mathematical reasoning [8, 35], and related work extends outcome-based RL to multimodal settings to couple perception with stepwise reasoning [50, 61]. Overall, reasoning benefits from data-centric SFT to bootstrap stepwise behavior and from outcome-based RL to move beyond imitation. However, many approaches still depend on reward models or human labels [22, 32], which are costly in specialized domains and hard to maintain after deployment, motivating methods that learn from verifiable signals with minimal supervision at test time.

2.2. Test-Time Scaling

Test-time scaling increases the compute budget at inference without updating model parameters. Prior work suggests that for many reasoning tasks, allocating extra compute at test-time can be more sample efficient than scaling pretraining compute [18, 26, 36]. Two common forms are parallel generation and sequential generation [51]. Paral-

lel generation draws multiple candidates or decision paths and then aggregates them, e.g., self-consistency and best of N [5, 30, 37, 47], Monte Carlo Tree Search for discrete decisions [53, 63], or token-level search, such as reward-guided sampling [19, 33]. Aggregation may rely on simple voting or reward models [22, 44, 62]. Sequential generation allocates more steps to a single response through reflection and chain-of-thought prompting [29, 48]. While these strategies improve accuracy, their gains are ultimately bounded by the base model and by the cost and latency of large-scale sampling. Beyond scaling inference-time sampling, test-time training (TTT) updates parameters on unlabeled inputs via pseudo-labels or self-supervision [1, 45]. Test-Time RL (TTRL) [67] instead uses majority-vote self-consistency as a verifiable reward, with MM-UPT extending to multimodal models [49]. ETTRL [25] reshapes rollouts and advantages via response-level entropy. Compute as Teacher (CaT) remains label-free but introduces an external teacher/judge (e.g., GPT-4o) to synthesize and verify answers [15], thus replacing self-consistency with auxiliary model feedback. EVOL-RL is likewise label-free yet relies on an external embedding model to score novelty and performs full-sequence policy updates guided by embedding similarity [64]. In contrast, our method avoids external teachers and embedders and operates at the token level. We update only high-entropy *forking tokens* and apply an entropy band with a masked KL at those positions, isolating the gains of selective token updates under a matched GRPO-style TTRL setup.

3. Methodology

Setting and notation. We study label-free test-time reinforcement learning for autoregressive reasoning models, including both text-only LLMs and multimodal LLMs

(MLLMs). Given an input x , the policy $\pi_\theta(y \mid x)$ generates $y = (a_1, \dots, a_T)$ autoregressively, where each token is sampled as $a_t \sim \pi_\theta(\cdot \mid s_t)$ and s_t denotes the decoder state before emitting token t (i.e., a summary of x and $a_{<t}$). All subsequent quantities (e.g., rewards, advantages, and entropies) are defined on the model’s output distributions and do not depend on the input modality.

At test-time, the model receives only unlabeled inputs and must improve its reasoning behavior without any ground-truth supervision. To this end, we leverage reinforcement learning with self-consistency rewards and grouped advantage estimation. Our key idea is to perform *token-selective test-time reinforcement learning*: we identify high-entropy forking tokens, where the chain-of-thought branches, and apply an entropy-band constraint that suppresses overly high entropy while preventing collapse, thereby stabilizing updates under noisy pseudo-rewards. This selective update mechanism, integrated with self-consistency rewards and the GRPO objective, forms the core of our SPINE.

3.1. Self-consistency reward and GRPO objective

Without ground-truth labels, we derive a verifiable supervision signal through self-consistency. For each input x , we draw N candidate responses $\{y_i\}_{i=1}^N \sim \pi_{\theta_{\text{old}}}(\cdot \mid x)$ and aggregate them into a consensus output y^* (e.g., majority voting over extracted answers). Each sampled response y_i then receives a rule-based reward

$$r_i = r(y_i, y^*) \in [0, 1] \quad (1)$$

such as exact agreement or a task-specific verifiable score (e.g., unit tests for code). When noted, we adopt a leave-one-out variant y_{-i}^* to mitigate self-inclusion bias. This self-consistency reward encourages the model to prefer stable, high-consensus reasoning paths without relying on external supervision.

To optimize the policy using these rewards, we adopt Grouped Relative Policy Optimization (GRPO), a stable on-policy reinforcement learning algorithm that replaces explicit value estimation with group-wise normalized advantages. Within each group of N samples for the same input x , the standardized advantage for the i -th sample is computed as

$$\hat{A}^i = \frac{r_i - \text{mean}(\{r_j\}_{j=1}^N)}{\text{std}(\{r_j\}_{j=1}^N) + \epsilon}, \quad i = 1, \dots, N \quad (2)$$

and the token-level PPO ratio is

$$\rho_t^{(i)}(\theta) = \frac{\pi_\theta(a_t^{(i)} \mid s_t^{(i)})}{\pi_{\theta_{\text{old}}}(a_t^{(i)} \mid s_t^{(i)})}. \quad (3)$$

The clipped surrogate objective is then

$$\ell_{\text{PPO}} = \min \left[\rho_t^{(i)} \hat{A}^i, \text{clip}(\rho_t^{(i)}, 1 - \epsilon, 1 + \epsilon) \hat{A}^i \right] \quad (4)$$

where the clip operator truncates the ratio to the interval $[1 - \epsilon, 1 + \epsilon]$.

To ensure stable adaptation without over-regularizing non-forking positions, we apply a token-level KL anchor only on forking tokens. Concretely, we define a masked, size-normalized KL term

$$\ell_{\text{KL}}^{\text{fork}} = \frac{\mathbb{E}_{(i,t) \in \mathcal{B}} [m_t^{(i)} D_{\text{KL}}(\pi_\theta(\cdot \mid s_t^{(i)}) \parallel \pi_{\text{ref}}(\cdot \mid s_t^{(i)}))]}{\mathbb{E}_{(i,t) \in \mathcal{B}} [m_t^{(i)}] + \epsilon}, \quad (5)$$

where π_{ref} denotes the fixed reference policy, set to the pre-adaptation base model π_{θ_0} and kept frozen throughout adaptation. Here $m_t^{(i)} \in \{0, 1\}$ masks the top-20% entropy forking tokens. This choice preserves flexibility on low-entropy, non-branching tokens while anchoring updates at high-uncertainty forks where policy drift is most likely.

3.2. Selecting forking tokens by entropy

Reward improvements in reasoning models are mainly concentrated at branching points of the chain-of-thought. We therefore identify such forking tokens through their token-level entropy, defined as

$$H_t = - \sum_{v \in \mathcal{V}} \pi_\theta(v \mid s_t) \log \pi_\theta(v \mid s_t), \quad (6)$$

which measures the uncertainty of the predictive distribution at step t . For each sampled output y_i , we compute $\{H_t^{(i)}\}_{t=1}^{T_i}$ and select the top 20% tokens with the highest entropy as the set of forking tokens $\mathcal{S}_i \subset \{1, \dots, T_i\}$. A binary mask $m_t^{(i)} \in \{0, 1\}$ marks these positions, and we ensure at least one token is always selected to avoid degenerate cases. These high-entropy tokens correspond to the model’s reasoning forks, where adaptation yields the largest expected reward gain.

3.3. Entropy-band regularization via quantiles

Building on the forking tokens \mathcal{S}_i defined above, we regularize their entropy distribution to avoid instability during adaptation. Uniform entropy maximization can lead to over-exploration, while entropy collapse prematurely prunes reasoning branches. We therefore shape token-level uncertainty only at forking points by constraining entropies to remain within a per-sample, data-driven band defined by fixed quantiles.

For each sample i , we collect the entropies of forking tokens $\{H_t^{(i)} : t \in \mathcal{S}_i\}$ and compute two fixed quantiles:

$$\begin{aligned} H_{\text{low}}^{(i)} &= \text{Quantile}_{10\%} \{H_t^{(i)} : t \in \mathcal{S}_i\}, \\ H_{\text{high}}^{(i)} &= \text{Quantile}_{50\%} \{H_t^{(i)} : t \in \mathcal{S}_i\}. \end{aligned} \quad (7)$$

The quantile band adapts automatically to each sample’s entropy distribution without requiring any task-specific tuning

Table 1. Performance of SPINE on multimodal reasoning and medical QA benchmarks. SPINE consistently improves over TTRL and the base model across both multimodal VQA tasks (MathVision, SLAKE, MedXpertQA-MM) and medical QA (MedQA, PubMedQA).

Name	MathVision	SLAKE	MedXpertQA-MM	MedQA	PubMedQA	Avg
Base Model	Qwen2.5-VL-3B-Instruct			Qwen3-1.7B		
No adaptation	19.65	26.17	17.17	30.40	68.00	32.28
Self-Consistency	19.20	25.84	19.47	39.62	68.42	34.51
w/ LMSI	9.21	9.05	22.01	50.47	71.20	32.39
w/ SEALONG	10.36	12.32	6.51	49.69	71.00	29.98
w/ TTRL	22.73	30.00	22.61	51.88	71.50	39.74
w/ SPINE	27.26	38.66	23.92	55.40	76.20	44.29
Δ	+4.5	+8.7	+1.3	+3.5	+4.7	+4.6

or scale parameters. It provides a simple, robust mechanism to prevent entropy collapse while allowing flexible exploration across reasoning paths.

The band statistics are treated as constants within each update; we denote the stop-gradient operator by $\text{sg}(\cdot)$ and write

$$\bar{H}_{\text{low}}^{(i)} := \text{sg}(H_{\text{low}}^{(i)}), \quad \bar{H}_{\text{high}}^{(i)} := \text{sg}(H_{\text{high}}^{(i)}). \quad (8)$$

Violations are penalized by hinge losses:

$$\ell_t^{\text{high}} = \max(0, H_t^{(i)} - \bar{H}_{\text{high}}^{(i)}), \quad \ell_t^{\text{low}} = \max(0, \bar{H}_{\text{low}}^{(i)} - H_t^{(i)}). \quad (9)$$

The overall band regularization aggregates these penalties only over forking tokens:

$$\mathcal{R}_{\text{band}}(\theta) = \mathbb{E}_{(i,t) \in \mathcal{B}} [(\beta_{\ell} \ell_t^{\text{low}} + \beta_u \ell_t^{\text{high}}) m_t^{(i)}]. \quad (10)$$

where ℓ_t^{high} and ℓ_t^{low} denote per-token penalties for excessive and insufficient entropy respectively, and $m_t^{(i)}$ masks forking tokens.

3.4. Final objective

We optimize the core loss over mini-batches of prompts, samples, and tokens:

$$\mathcal{L}_{\text{core}} = -\mathbb{E}_{(i,t) \in \mathcal{B}} [m_t^{(i)} \ell_{\text{PPO}}] + \lambda_{\text{KL}} \ell_{\text{KL}}^{\text{fork}}, \quad (11)$$

and add the entropy-band regularizer $\mathcal{R}_{\text{band}}$ defined in Eq. (10), whose strength is controlled by β_{ℓ} and β_u . The final objective is

$$\mathcal{L} = \mathcal{L}_{\text{core}} + \mathcal{R}_{\text{band}}. \quad (12)$$

Test-time update loop. For each unlabeled input x : (i) sample N responses with the behavior policy $\pi_{\theta_{\text{old}}}$; (ii) aggregate to a consensus y^* and compute rule-based rewards $\{r_i\}$; (iii) compute grouped, standardized advantages $\{\hat{A}^i\}$ by Eq. (2); (iv) compute token entropies $\{H_t^{(i)}\}$, select forking tokens (top-20% per sample) to obtain masks $m_t^{(i)}$, and compute the per-sample quantile thresholds by Eq. (7); (v) update θ by minimizing Eq. (12). Repeat the loop for a small number of iterations over the test split.

4. Experiments

4.1. Experimental Setup

Models We evaluate SPINE on a compact, representative suite spanning multimodal and text-only LLMs, covering model type (MLLM vs. LLM), specialization (generalist vs. math-focused), and scale (1.5–3B). Concretely, we use Qwen2.5-VL-3B-Instruct for multimodal reasoning [55], Qwen3-1.7B as a general-purpose text-only LLM [57], and Qwen2.5-Math-1.5B as a math-specialized LLM [56]. Experiments initialize from publicly released checkpoints.

Benchmarks We evaluate SPINE across four task families. For multimodal VQA, we consider MathVision [43] for diagram-based mathematical reasoning, as well as SLAKE [23] and MedXpertQA-MM [66] for clinical image understanding. For general and expert knowledge QA, we include GPQA [34] and MMLU [9]. For mathematical reasoning, we use AIME 2025, AMC, and the MATH-500 subset of MATH [10]. For medical text-only QA, we adopt MedQA (USMLE) [16] and PubMedQA [17].

Baselines We use standard TTRL (GRPO with a KL anchor and majority-vote self-consistency) [67] as our primary baseline, and additionally report No adaptation and Self-Consistency (majority vote without updates). For broader comparison, we include two self-improvement baselines: LMSI [13], which generates high-confidence CoT pseudo-labels via self-consistency and performs supervised fine-tuning; and SEALONG [21], which samples multiple long-context trajectories, scores them via MBR-style consensus, and fine-tunes on the top outputs.

Implementation Details and Evaluation Protocol We implement SPINE with GRPO on all benchmarks. During adaptation, for each prompt we sample $N=8$ rollouts with temperature 0.7 and top- $p=0.95$, aggregate a pseudo-label via self-consistency (majority vote), and update the policy using GRPO with an optional KL anchor to the base

Table 2. Performance of SPINE on mathematical, general, and expert reasoning benchmarks. SPINE consistently outperforms both TTRL and the base model across mathematical tasks (AIME 2025, AMC, MATH-500) and general or expert benchmarks (GPQA, MMLU).

Name	AIME 2025	AMC	MATH-500	GPQA	MMLU	Avg
Base Model	Qwen2.5-Math-1.5B					
No adaptation	10.00	28.91	30.20	4.06	-	18.29
Self-Consistency	3.33	31.02	45.37	6.15	-	21.47
w/ LMSI	6.67	26.50	31.50	19.19	-	20.97
w/ SEALONG	6.67	25.30	32.60	18.69	-	20.82
w/ TTRL	16.67	49.88	66.42	25.38	-	39.59
w/ SPINE	20.00	59.03	77.00	30.96	-	46.75
Δ	+3.3	+9.2	+10.6	+5.6	-	+7.2
Base Model	Qwen3-1.7B					
No adaptation	10.00	38.55	71.60	9.09	58.16	37.48
Self-Consistency	10.83	33.13	66.07	8.75	65.39	36.83
w/ LMSI	16.67	34.94	62.40	18.18	71.74	40.78
w/ SEALONG	20.00	40.96	61.00	13.64	69.36	40.99
w/ TTRL	26.67	53.01	79.86	29.94	71.19	52.13
w/ SPINE	36.67	61.46	81.40	36.04	72.66	57.65
Δ	+10.0	+8.5	+1.5	+6.1	+1.5	+5.5

Table 3. Cross-Task Generalization of SPINE based on Qwen3-1.7B. Each model is adapted on one dataset and evaluated across all four benchmarks to measure generalization and forgetting.

Training	AIME 2025	AMC	MATH-500	GPQA	Avg
Qwen3-1.7B	10.00	38.55	71.60	9.09	32.31
AIME 2025	36.67	48.19	78.60	24.36	46.96
Δ	+26.7	+9.6	+7.0	+15.3	+14.7
AMC	20.00	61.46	76.40	22.84	45.18
Δ	+10.0	+22.9	+4.8	+13.8	+12.9
MATH-500	23.33	49.39	81.40	18.78	43.23
Δ	+13.3	+10.8	+9.8	+9.7	+10.9
GPQA	10.00	40.96	70.00	36.04	39.25
Δ	+0.0	+2.4	-1.6	+27.0	+6.9

model. At evaluation, we use greedy decoding (temperature 0) and report Pass@1 accuracy (a single greedy output). Predictions are matched to references after a standard normalization pipeline, case folding, whitespace cleanup, Unicode/LaTeX canonicalization (including symbol mapping), unit-word removal, mixed-number handling, and algebraic equivalence checking via `sympy` when applicable; full rules follow the `grade_answer` implementation. We set the maximum output length to 3072 tokens for LLM tasks and 2048 tokens for multimodal tasks, and keep sampling filters and stopping criteria identical across methods. For multimodal models, following MM-UPT [49], we do not freeze the vision tower during training. All runs use a fixed seed for reproducibility and are conducted on 4×NVIDIA A100 80GB GPUs. For fair comparison, all experiments are conducted using the EasyR1 framework [58] under a unified configuration. Except for the hyperparameters specific to our method, all other training settings are

kept identical across experiments. With matched compute budgets, SPINE exhibits broadly comparable efficiency to TTRL.

4.2. Main Results

Results on multimodal VQA tasks. Table 1 shows that TTRL improves the no-adaptation baseline on MathVision, SLAKE, and MedXpertQA-MM from 19.65/26.17/17.17 to 22.73/30.00/22.61. Building on this, SPINE reaches 27.26/38.66/23.92, which is +4.5, +8.7, and +1.3 over TTRL. In contrast, recent SFT-based methods such as LMSI and SEALONG do not exhibit clear improvements and even lead to declines on certain benchmarks, highlighting the limited generalization of supervised fine-tuning under unseen multimodal distributions.

Results on mathematical reasoning tasks. Table 2 reports results on three mathematical benchmarks. On Qwen2.5-Math-1.5B, TTRL improves the no-adaptation baseline from 10.00 to 16.67 on AIME 2025, from 28.91 to 49.88 on AMC, and from 30.20 to 66.42 on MATH-500. SPINE further increases the scores to 20.00, 59.03, and 77.00, giving additional gains of 3.3, 9.2, and 10.6. A similar pattern appears on Qwen3-1.7B, where SPINE reaches 36.67 on AIME 2025, 61.46 on AMC, and 81.40 on MATH-500, improving over TTRL by 10.0, 8.5, and 1.5. In contrast, SFT-based approaches such as LMSI and SEALONG show mild improvements over the baseline.

Table 4. Ablation study of SPINE. **FT**: selective update on Forking Tokens; **EB**: Entropy-Band regularization. Both modules consistently improve TTRL across benchmarks.

Method	MathVision	SLAKE	GPQA	Avg
Base	19.65	26.17	9.09	18.30
+TTRL	22.73	30.00	29.94	27.56
Δ vs. Base	+3.1	+3.8	+20.9	+9.3
+TTRL+FT	25.12	32.66	34.51	30.76
Δ vs. Base	+5.5	+6.5	+25.4	+12.5
+TTRL+FT+EB	27.26	38.66	36.04	33.99
Δ vs. Base	+7.6	+12.5	+27.0	+15.7

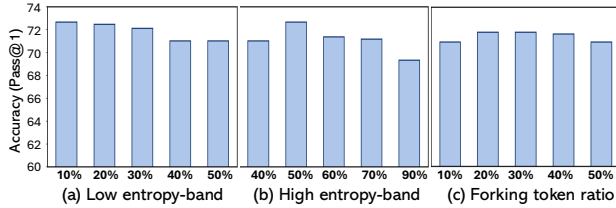


Figure 3. Hyperparameter sensitivity: (a–b) show the effect of varying the lower and upper quantiles of the entropy band, while (c) varying the forking-token ratio on MMLU.

Results on medical and general reasoning tasks. Table 1 and Table 2 also show the results on medical QA and general reasoning benchmarks. On domain-specific medical tasks, TTRL improves over the no-adaptation baseline, and SPINE further increases accuracy to 55.40 on MedQA and 76.20 on PubMedQA, adding 3.5 and 4.7 points over TTRL. On general and expert reasoning tasks, SPINE also brings consistent gains. With Qwen3-1.7B, it raises GPQA from 29.94 to 36.04 and MMLU from 71.19 to 72.66, corresponding to improvements of 6.1 and 1.5. These results indicate that selective token updates with entropy-band regularization yield more stable and accurate adaptation than TTRL.

SPINE generalizes well beyond the target task. To assess whether SPINE overfits the adaptation dataset or loses generalization on unseen domains, we conduct a cross-task evaluation on four benchmarks. Table 3 shows that adapting on AIME 2025 raises the average Pass@1 from 32.31 to 46.96, with consistent gains on AMC, MATH-500, and GPQA. Adapting on AMC and MATH-500 shows a similar pattern, yielding improvements across tasks with average gains of +12.9 and +10.9, respectively. Adapting on GPQA leads to a strong in-domain improvement of 27.0 and stable results on AIME 2025 and AMC, with only a small decline of 1.6 on MATH-500. These findings show that SPINE generalizes well across tasks under label-free adaptation.

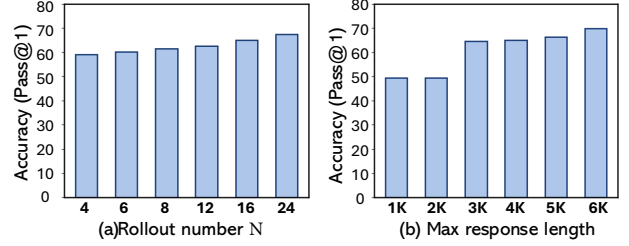


Figure 4. Sensitivity to scaling-related hyperparameters, with larger rollout N and longer response lengths providing consistent improvements on the challenging AIME 2025.

4.3. Ablation Study

Component Analysis. Table 4 reports the ablation results of SPINE. Starting from TTRL, which improves the base model by 9.3 on average, adding the Forking Token module brings further gains, increasing the average accuracy from 27.56 to 30.76. Entropy-Band regularization provides additional stability and raises the average to 33.99. Together, FT and EB achieve the best results, with an overall improvement of 15.7 over the base model and 6.4 over TTRL. These findings show that selective token updates and entropy-aware regularization reinforce each other and substantially enhance adaptation quality.

Hyperparameter Sensitivity Analysis. Since SPINE operates at test time, practical deployments typically cannot tune hyperparameters for each input. We therefore adopt a single configuration across all experiments and assess robustness to key hyperparameters. Figure 3 reports results on MMLU, varying (a) the lower quantile of the entropy band (with the upper bound fixed to the median), (b) the upper quantile of the entropy band, and (c) the forking-token ratio. Performance shows limited variation across settings, with a mild preference for a 0.10 lower quantile, a 0.50 upper quantile, and a forking-token ratio near 20%, confirming the robustness of SPINE under different configurations.

To further assess scaling behavior, Figure 4 varies the rollout number N and the maximum response length on the challenging AIME 2025. Accuracy improves steadily as more test-time compute is allocated, while avoiding marked degradation under modest compute budgets.

5. Analysis and Discussions

5.1. Training Dynamics

Beyond the failure cases in Fig. 1b, we analyze TTRL’s instability in Fig. 5. As training proceeds, the majority-vote reward of TTRL quickly saturates at 1.0, indicating overfitting to pseudo-consensus and loss of reasoning diversity. In contrast, SPINE shows a slower, bounded increase, maintaining multiple reasoning trajectories. Likewise, TTRL’s

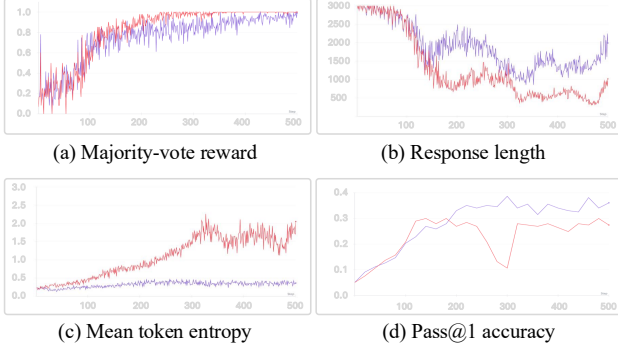


Figure 5. Training dynamics comparison between SPINE (blue) and TTRL (red) on GPQA. (a) Majority-vote reward, (b) response length, (c) mean token entropy, and (d) Pass@1 accuracy.

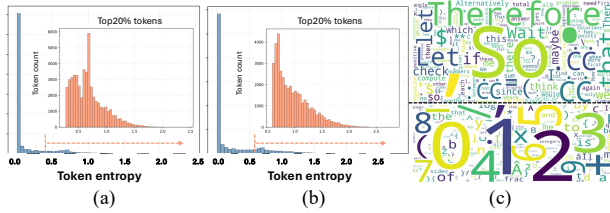


Figure 6. Token entropy analysis before (a) and after (b) adaptation with SPINE. Panel (c) highlights their semantic differences: the upper word cloud shows high-entropy tokens, while the lower one corresponds to low-entropy tokens.

response length drops sharply, while SPINE shows only mild shortening, suggesting its reasoning chains remain active. Token-level entropy in Fig. 5c shows that TTRL’s uncertainty grows erratically, whereas SPINE keeps it nearly steady, reflecting more stable reasoning. Finally, Fig. 5d shows that SPINE achieves consistently higher and more stable Pass@1 accuracy as training continues.

5.2. Entropy Distribution and Forking Tokens

We examine token-level entropy before and after adaptation in Fig. 6. At initialization (a), most tokens are low-entropy with a small high-entropy tail. After adapting with SPINE (b), this shape remains, indicating stable uncertainty without collapse or over-dispersion. We further visualize the top 20% high-entropy tokens (c); despite some overlap with frequent words, they more often correspond to branching cues that steer diverse reasoning, supporting our use of entropy-guided updates.

5.3. Why Does SPINE Work?

Self-consistency offers a verifiable test-time reward: drawing multiple rollouts raises the chance that at least one is correct, and small online updates steer the policy toward consensus without labels. SPINE improves both where and how to update. First, Forking-Token (FT) selective updates focus gradients on decision-critical tokens identified by en-

tropy and branch structure, so learning targets tokens that change the final answer rather than boilerplate, reducing reward overfitting and preserving alternative paths. Second, Entropy-Band (EB) regularization keeps token-level uncertainty within a target band, preventing low-entropy collapse and high-entropy drift, thereby stabilizing trajectory distributions. Empirically, these choices yield bounded reward growth, milder response-length shrinkage, stable token-entropy, and higher Pass@1 than uniform TTRL updates.

5.4. Limitations and Failure Modes

Although SPINE improves accuracy even when the initial majority-vote accuracy is below 0.5, it can still struggle under severe domain mismatch where the model’s prior is systematically wrong and the consensus is consistently incorrect. In such cases, the pseudo-reward provides little corrective signal and adaptation may reinforce spurious reasoning patterns. Moreover, when the underlying task requires structured or multi-hop reasoning that substantially deviates from the model’s pretraining distribution, the benefits of selective updates diminish because the branching structure itself becomes unreliable. Finally, test-time training introduces additional computational overhead, which may limit deployment in strict latency-constrained environments.

6. Conclusion

In this paper, we introduced SPINE, a selective test-time reinforcement learning framework that aligns updates with decision-critical (forking) tokens and stabilizes adaptation via an entropy-band constraint. Built on self-consistency rewards and GRPO, SPINE requires no ground-truth labels and retains comparable efficiency to standard TTRL under matched compute budgets. Across ten benchmarks spanning multimodal VQA, general and expert QA, mathematical reasoning, and medical QA, SPINE consistently outperforms TTRL and no-adaptation baselines in practice while robustly avoiding majority-vote saturation, response-length collapse, and entropy drift. Empirically, analyses of training dynamics and token-entropy distributions indicate that SPINE preserves diverse reasoning trajectories and concentrates learning where it most affects the answer.

References

- [1] Ekin Akyürek, Mehul Damani, Linlu Qiu, Han Guo, Yoon Kim, Andreas, and Jacob. The surprising effectiveness of test-time training for abstract reasoning. *arXiv preprint*, 2024. 1, 3
- [2] Ali Behrouz, Peilin Zhong, Mirrokni, and Vahab. Titans: Learning to memorize at test time. *arXiv preprint*, 2024. 1
- [3] Stephen Casper, Xander Davies, Claudia Shi, Thomas Krendl Gilbert, Jérémy Scheurer, Javier Rando, Rachel Freedman, Tomasz Korbak, David Lindner, Pedro

- Freire, et al. Open problems and fundamental limitations of reinforcement learning from human feedback. *arXiv preprint arXiv:2307.15217*, 2023. 1
- [4] Qiguang Chen, Libo Qin, Jinhao Liu, Dengyun Peng, Jian-nan Guan, Peng Wang, Mengkang Hu, Yuhang Zhou, Te Gao, and Wanxiang Che. Towards reasoning era: A survey of long chain-of-thought for reasoning large language models. *arXiv preprint arXiv:2503.09567*, 2025. 3
- [5] Xinyun Chen, Renat Aksitov, Uri Alon, Jie Ren, Kefan Xiao, Pengcheng Yin, Sushant Prakash, Charles Sutton, Xuezhi Wang, Zhou, and Denny. Universal self-consistency for large language model generation. *arXiv preprint*, 2023. 3
- [6] Hyung Won Chung, Le Hou, Shayne Longpre, Barret Zoph, Yi Tay, William Fedus, Yunxuan Li, Xuezhi Wang, Mostafa Dehghani, Siddhartha Brahma, et al. Scaling instruction-finetuned language models. *Journal of Machine Learning Research*, 25(70):1–53, 2024. 2
- [7] Dylan J Foster, Adam Block, and Dipendra Misra. Is behavior cloning all you need? understanding horizon in imitation learning. *Advances in Neural Information Processing Systems*, 37:120602–120666, 2024. 3
- [8] Daya Guo, Dejian Yang, Haowei Zhang, Junxiao Song, Ruoyu Zhang, Runxin Xu, Qihao Zhu, Shirong Ma, Peiyi Wang, Xiao Bi, and et al. Deepseek-r1: Incentivizing reasoning capability in llms via reinforcement learning. *arXiv preprint*, 2025. 1, 3
- [9] Dan Hendrycks, Collin Burns, Steven Basart, Andy Zou, Mantas Mazeika, Dawn Song, and Jacob Steinhardt. Measuring massive multitask language understanding. *arXiv preprint arXiv:2009.03300*, 2020. 5
- [10] Dan Hendrycks, Collin Burns, Saurav Kadavath, Akul Arora, Steven Basart, Eric Tang, Dawn Song, Steinhardt, and Jacob. Measuring mathematical problem solving with the math dataset. *arXiv preprint*, 2021. 5
- [11] Jinwu Hu, Zhitian Zhang, Guohao Chen, Xutao Wen, Chao Shuai, Wei Luo, Bin Xiao, Yuanqing Li, and Mingkui Tan. Test-time learning for large language models. *arXiv preprint arXiv:2505.20633*, 2025. 1
- [12] Ming Hu, Chenglong Ma, Wei Li, Wanghan Xu, Jiamin Wu, Jucheng Hu, Tianbin Li, Guohang Zhuang, Jiaqi Liu, Yingzhou Lu, et al. A survey of scientific large language models: From data foundations to agent frontiers. *arXiv preprint arXiv:2508.21148*, 2025. 1
- [13] Jiaxin Huang, Shixiang Gu, Le Hou, Yuexin Wu, Xuezhi Wang, Hongkun Yu, and Jiawei Han. Large language models can self-improve. In *Proceedings of the 2023 conference on empirical methods in natural language processing*, pages 1051–1068, 2023. 5
- [14] Aaron Jaech, Adam Kalai, Adam Lerer, Adam Richardson, Ahmed El-Kishky, Aiden Low, Alec Helyar, Aleksander Madry, Alex Beutel, Alex Carney, and et al. Openai o1 system card. *arXiv preprint*, 2024. 1
- [15] Dulhan Jayalath, Shashwat Goel, Thomas Foster, Parag Jain, Suchin Gururangan, Cheng Zhang, Anirudh Goyal, and Alan Schelten. Compute as teacher: Turning inference compute into reference-free supervision. *arXiv preprint arXiv:2509.14234*, 2025. 3
- [16] Di Jin, Eileen Pan, Nassim Oufattole, Wei-Hung Weng, Hanyi Fang, and Peter Szolovits. What disease does this patient have? A large-scale open domain question answering dataset from medical exams. *Applied Sciences*, 11(14):6421, 2021. 5
- [17] Qiao Jin, Bhuwan Dhingra, Zhengping Liu, William W Cohen, and Xinghua Lu. PubMedQA: A dataset for biomedical research question answering. *arXiv preprint arXiv:1909.06146*, 2019. 5
- [18] Jared Kaplan, Sam McCandlish, Tom Henighan, Tom B Brown, Benjamin Chess, Rewon Child, Scott Gray, Alec Radford, Jeffrey Wu, and Dario Amodei. Scaling laws for neural language models. *arXiv preprint arXiv:2001.08361*, 2020. 3
- [19] Maxim Khanov, Jirayu Burapachee, Li, and Yixuan. Args: Alignment as reward-guided search. *arXiv preprint*, 2024. 3
- [20] Hung Le, Yue Wang, Akhilesh Deepak Gotmare, Silvio Savarese, and Steven Chu Hong Hoi. Coder1: Mastering code generation through pretrained models and deep reinforcement learning. *Advances in Neural Information Processing Systems*, 35:21314–21328, 2022. 3
- [21] Siheng Li, Cheng Yang, Zesen Cheng, Lemao Liu, Mo Yu, Yujiu Yang, and Wai Lam. Large language models can self-improve in long-context reasoning. *arXiv preprint arXiv:2411.08147*, 2024. 5
- [22] Hunter Lightman, Vineet Kosaraju, Yuri Burda, Harrison Edwards, Bowen Baker, Teddy Lee, Jan Leike, John Schulman, Ilya Sutskever, and Karl Cobbe. Let’s verify step by step. In *The Twelfth International Conference on Learning Representations*, 2023. 1, 3
- [23] Bo Liu, Li-Ming Zhan, Li Xu, Lin Ma, Yan Yang, and Xiao-Ming Wu. Slake: A semantically-labeled knowledge-enhanced dataset for medical visual question answering. In *2021 IEEE 18th international symposium on biomedical imaging (ISBI)*, pages 1650–1654. IEEE, 2021. 5
- [24] Haotian Liu, Chunyuan Li, Qingyang Wu, and Yong Jae Lee. Visual instruction tuning. *Advances in neural information processing systems*, 36:34892–34916, 2023. 3
- [25] Jia Liu, ChangYi He, YingQiao Lin, MingMin Yang, FeiYang Shen, and ShaoGuo Liu. Ettl: Balancing exploration and exploitation in llm test-time reinforcement learning via entropy mechanism. *arXiv preprint arXiv:2508.11356*, 2025. 3
- [26] Runze Liu, Junqi Gao, Jian Zhao, Kaiyan Zhang, Xiu Li, Biqing Qi, Wanli Ouyang, Zhou, and Bowen. Can 1b llm surpass 405b llm? rethinking compute-optimal test-time scaling. *arXiv preprint*, 2025. 3
- [27] Yixin Liu, Avi Singh, C Daniel Freeman, John D Co-Reyes, and Peter J Liu. Improving large language model fine-tuning for solving math problems. *arXiv preprint arXiv:2310.10047*, 2023. 1
- [28] Zhiyuan Liu, Yuting Zhang, Feng Liu, Changwang Zhang, Ying Sun, and Jun Wang. Othink-mr1: Stimulating multimodal generalized reasoning capabilities via dynamic reinforcement learning. *arXiv preprint arXiv:2503.16081*, 2025. 1
- [29] Aman Madaan, Niket Tandon, Prakhar Gupta, Skyler Hallinan, Luyu Gao, Sarah Wiegrefe, Uri Alon, Nouha Dziri,

- Shrimai Prabhumoye, Yiming Yang, and et al. Self-refine: Iterative refinement with self-feedback. *Advances in Neural Information Processing Systems*, 36:46534–46594, 2023. 3
- [30] Reiichiro Nakano, Jacob Hilton, Suchir Balaji, Jeff Wu, Long Ouyang, Christina Kim, Christopher Hesse, Shantanu Jain, Vineet Kosaraju, William Saunders, et al. Webgpt: Browser-assisted question-answering with human feedback. *arXiv preprint arXiv:2112.09332*, 2021. 3
- [31] Changdae Oh, Zhen Fang, Shawn Im, Xuefeng Du, and Yixuan Li. Understanding multimodal llms under distribution shifts: An information-theoretic approach. *arXiv preprint arXiv:2502.00577*, 2025. 1
- [32] Long Ouyang, Jeffrey Wu, Xu Jiang, Diogo Almeida, Carroll Wainwright, Pamela Mishkin, Chong Zhang, Sandhini Agarwal, Katarina Slama, Alex Ray, and et al. Training language models to follow instructions with human feedback. *Advances in neural information processing systems*, 35:27730–27744, 2022. 3
- [33] Haikang Deng Raffel and Colin. Reward-augmented decoding: Efficient controlled text generation with a unidirectional reward model. *arXiv preprint*, 2023. 3
- [34] David Rein, Betty Li Hou, Asa Cooper Stickland, Jackson Petty, Richard Yuanzhe Pang, Julien Dirani, Julian Michael, Bowman, and Samuel R. Gpqa: A graduate-level google-proof q&a benchmark. *In First Conference on Language Modeling*, 2024. 5
- [35] Zhihong Shao, Peiyi Wang, Qihao Zhu, Runxin Xu, Junxiao Song, Xiao Bi, Haowei Zhang, Mingchuan Zhang, YK Li, Yang Wu, et al. Deepseekmath: Pushing the limits of mathematical reasoning in open language models. *arXiv preprint arXiv:2402.03300*, 2024. 1, 3
- [36] Charlie Snell, Jaehoon Lee, Kelvin Xu, Kumar, and Aviral. Scaling llm test-time compute optimally can be more effective than scaling model parameters. *arXiv preprint*, 2024. 3
- [37] Nisan Stiennon, Long Ouyang, Jeffrey Wu, Daniel Ziegler, Ryan Lowe, Chelsea Voss, Alec Radford, Dario Amodei, Christiano, and Paul F. Learning to summarize with human feedback. *Advances in neural information processing systems*, 33:3008–3021, 2020. 3
- [38] Yu Sun, Xiaolong Wang, Zhuang Liu, John Miller, Alexei A Efros, Hardt, and Moritz. Test-time training for out-of-distribution generalization. *Arxiv*, 2019. 1
- [39] Yu Sun, Xinhao Li, Karan Dalal, Jiarui Xu, Arjun Vikram, Genghan Zhang, Yann Dubois, Xinlei Chen, Xiaolong Wang, Sanmi Koyejo, and et al. Learning to (learn at test time): Rnns with expressive hidden states. *arXiv preprint*, 2024. 1
- [40] David Silver Sutton and Richard S. Welcome to the era of experience. *Google AI*, 2025. 1
- [41] Miles Turpin, Julian Michael, Ethan Perez, and Samuel Bowman. Language models don’t always say what they think: Unfaithful explanations in chain-of-thought prompting. *Advances in Neural Information Processing Systems*, 36:74952–74965, 2023. 3
- [42] Haochun Wang, Chi Liu, Nuwa Xi, Zewen Qiang, Sendong Zhao, Bing Qin, and Ting Liu. Huatuo: Tuning llama model with chinese medical knowledge. *arXiv preprint arXiv:2304.06975*, 2023. 1
- [43] Ke Wang, Junting Pan, Weikang Shi, Zimu Lu, Houxing Ren, Aojun Zhou, Mingjie Zhan, and Hongsheng Li. Measuring multimodal mathematical reasoning with math-vision dataset. *Advances in Neural Information Processing Systems*, 37:95095–95169, 2024. 5
- [44] Peiyi Wang, Lei Li, Zhihong Shao, RX Xu, Damai Dai, Yifei Li, Deli Chen, Yu Wu, Sui, and Zhifang. Math-shepherd: Verify and reinforce llms step-by-step without human annotations. *arXiv preprint*, 2023. 3
- [45] Renhao Wang, Yu Sun, Arnub Tandon, Yossi Gandelsman, Xinlei Chen, Alexei A Efros, and Xiaolong Wang. Test-time training on video streams. *Journal of Machine Learning Research*, 26(9):1–29, 2025. 3
- [46] Shenzhi Wang, Le Yu, Chang Gao, Chujie Zheng, Shixuan Liu, Rui Lu, Kai Dang, Xionghui Chen, Jianxin Yang, Zhenru Zhang, et al. Beyond the 80/20 rule: High-entropy minority tokens drive effective reinforcement learning for llm reasoning. *arXiv preprint arXiv:2506.01939*, 2025. 1
- [47] Xuezhi Wang, Jason Wei, Dale Schuurmans, Quoc Le, Ed Chi, Sharan Narang, Aakanksha Chowdhery, Zhou, and Denny. Self-consistency improves chain of thought reasoning in language models. *arXiv preprint*, 2022. 2, 3
- [48] Jason Wei, Xuezhi Wang, Dale Schuurmans, Maarten Bosma, Fei Xia, Ed Chi, Quoc V Le, Denny Zhou, et al. Chain-of-thought prompting elicits reasoning in large language models. *Advances in neural information processing systems*, 35:24824–24837, 2022. 1, 2, 3
- [49] Lai Wei, Yuting Li, Chen Wang, Yue Wang, Linghe Kong, Weiran Huang, and Lichao Sun. Unsupervised post-training for multi-modal llm reasoning via grp. *arXiv preprint arXiv:2505.22453*, 2025. 1, 3, 6
- [50] Lai Wei, Yuting Li, Kaipeng Zheng, Chen Wang, Yue Wang, Linghe Kong, Lichao Sun, and Weiran Huang. Advancing multimodal reasoning via reinforcement learning with cold start. *arXiv preprint arXiv:2505.22334*, 2025. 3
- [51] Sean Welleck, Amanda Bertsch, Matthew Finlayson, Haley Schoelkopf, Alex Xie, Graham Neubig, Ilia Kulikov, Harchaoui, and Zaid. From decoding to meta-generation: Inference-time algorithms for large language models. *arXiv preprint*, 2024. 3
- [52] Yongliang Wu, Yizhou Zhou, Zhou Ziheng, Yingzhe Peng, Xinyu Ye, Xinting Hu, Wenbo Zhu, Lu Qi, Ming-Hsuan Yang, and Xu Yang. On the generalization of sft: A reinforcement learning perspective with reward rectification. *arXiv preprint arXiv:2508.05629*, 2025. 1
- [53] Yuxi Xie, Anirudh Goyal, Wenyue Zheng, Min-Yen Kan, Timothy P Lillicrap, Kenji Kawaguchi, Shieh, and Michael. Monte carlo tree search boosts reasoning via iterative preference learning. *arXiv preprint*, 2024. 3
- [54] Guowei Xu, Peng Jin, Ziang Wu, Hao Li, Yibing Song, Lichao Sun, and Li Yuan. Llava-cot: Let vision language models reason step-by-step. In *Proceedings of the IEEE/CVF International Conference on Computer Vision*, pages 2087–2098, 2025. 3
- [55] An Yang, Baosong Yang, Beichen Zhang, Binyuan Hui, Bo Zheng, Bowen Yu, Chengyuan Li, Dayiheng Liu, Fei Huang, Haoran Wei, Huan Lin, Jian Yang, Jianhong Tu, Jianwei

- Zhang, Jianxin Yang, Jiayi Yang, Jingren Zhou, Junyang Lin, Kai Dang, Keming Lu, Keqin Bao, Kexin Yang, Le Yu, Mei Li, Mingfeng Xue, Pei Zhang, Qin Zhu, Rui Men, Runji Lin, Tianhao Li, Tingyu Xia, Xingzhang Ren, Xuancheng Ren, Yang Fan, Yang Su, Yichang Zhang, Yu Wan, Yuqiong Liu, Zeyu Cui, Zhenru Zhang, Qiu, and Zihan. Qwen2.5 technical report. *arXiv preprint*, 2024. 5
- [56] An Yang, Beichen Zhang, Binyuan Hui, Bofei Gao, Bowen Yu, Chengpeng Li, Dayiheng Liu, Jianhong Tu, Jingren Zhou, Junyang Lin, et al. Qwen2. 5-math technical report: Toward mathematical expert model via self-improvement. *arXiv preprint arXiv:2409.12122*, 2024. 5
- [57] An Yang, Anfeng Li, Baosong Yang, Beichen Zhang, Binyuan Hui, Bo Zheng, Bowen Yu, Chang Gao, Chengen Huang, Chenxu Lv, et al. Qwen3 technical report. *arXiv preprint arXiv:2505.09388*, 2025. 5
- [58] Shenzhi Wang, Zhangchi Feng, Dongdong Kuang, Yuwen Xiong, Yaowei Zheng, Junting Lu. Easyrl: An efficient, scalable, multi-modality rl training framework. <https://github.com/hiyouga/EasyR1>, 2025. 6
- [59] Lifan Yuan, Yangyi Chen, Ganqu Cui, Hongcheng Gao, Fangyuan Zou, Xingyi Cheng, Heng Ji, Zhiyuan Liu, and Maosong Sun. Revisiting out-of-distribution robustness in nlp: Benchmarks, analysis, and llms evaluations. *Advances in Neural Information Processing Systems*, 36:58478–58507, 2023. 1
- [60] Eric Zelikman, Yuhuai Wu, Jesse Mu, and Noah Goodman. Star: Bootstrapping reasoning with reasoning. *Advances in Neural Information Processing Systems*, 35:15476–15488, 2022. 2
- [61] Jingyi Zhang, Jiaxing Huang, Huanjin Yao, Shunyu Liu, Xikun Zhang, Shijian Lu, and Dacheng Tao. R1-vl: Learning to reason with multimodal large language models via step-wise group relative policy optimization. *arXiv preprint arXiv:2503.12937*, 2025. 3
- [62] Kaiyan Zhang, Jiayuan Zhang, Haoxin Li, Xuekai Zhu, Ermo Hua, Xingtai Lv, Ning Ding, Biqing Qi, and Bowen Zhou. Openprm: Building open-domain process-based reward models with preference trees. In *The Thirteenth International Conference on Learning Representations*, 2025. 3
- [63] Andy Zhou, Kai Yan, Michal Shlapentokh-Rothman, Hao-han Wang, Wang, and Yu-Xiong. Language agent tree search unifies reasoning acting and planning in language models. *arXiv preprint*, 2023. 3
- [64] Yujun Zhou, Zhenwen Liang, Haolin Liu, Wenhao Yu, Kishan Panaganti, Linfeng Song, Dian Yu, Xiangliang Zhang, Haitao Mi, and Dong Yu. Evolving language models without labels: Majority drives selection, novelty promotes variation. *arXiv preprint arXiv:2509.15194*, 2025. 3
- [65] Deyao Zhu, Jun Chen, Xiaoqian Shen, Xiang Li, and Mohamed Elhoseiny. Minigpt-4: Enhancing vision-language understanding with advanced large language models. *arXiv preprint arXiv:2304.10592*, 2023. 3
- [66] Yuxin Zuo, Shang Qu, Yifei Li, Zhangren Chen, Xuekai Zhu, Ermo Hua, Kaiyan Zhang, Ning Ding, and Bowen Zhou. Medxpertqa: Benchmarking expert-level medical reasoning and understanding. *arXiv preprint arXiv:2501.18362*, 2025. 5
- [67] Yuxin Zuo, Kaiyan Zhang, Li Sheng, Shang Qu, Ganqu Cui, Xuekai Zhu, Haozhan Li, Yuchen Zhang, Xinwei Long, Ermo Hua, et al. Ttrl: Test-time reinforcement learning. *arXiv preprint arXiv:2504.16084*, 2025. 1, 3, 5